Identification of a planar crack in Zener type viscoelasticity

Hui Duong Bui, Stéphanie Chaillat, Andrei Constantinescu, Eva Grasso

Identification of a planar crack in Zener type viscoelasticity

H. D. Bui · S. Chaillat · A. Constantinescu · E. Grasso

Abstract The paper addresses the identification of a planar crack for Zener type linear viscoelastic solids. Under the condition of low frequency, the Zener model of viscoelasticity establishes the equivalence between viscoelasticity and elasticity and the equations are reduced to a Helmholtz type problem for time harmonic loadings. The solutions to the crack identification problems are then obtained from the corresponding solutions in elasticity, using only one frequency.

Keywords Viscoelasticity · Crack identification · Inverse problems · Elastodynamics

1 Introduction

Inverse problems for defects identification in viscoelastic materials arise in different domains of applications like medicine, composite materials, geology, etc. In medical applications elastography techniques for detecting breast cancer (see [29]) benefit from recent progress in data measurements and computational inversion of equations. In aerospace applications, composite materials which are considered for their viscoelastic behaviour also present cracks as a consequence of delamination at the interface of laminates. The identification of these cracks is also a difficult problem.

Within the variety of viscoelastic materials models, there is always a difficulty when dealing with application, which is the choice of constitutive model which is close to reality and permits easy and robust identification. Within the class of generalized spring-dashpot models (see [19, 30]) we can cite the models of Voigt, Maxwell and Zener.

Most works consider simple models for the inversion, for example Voigt's model described by a linear relation between stress, strain and strain rate and loadings such as antiplane shear under the assumption of an unbounded solid. For example in [29] plane shear waves are used and finally a numerical inversion of the derived scalar Helmholtz conducts to the solution.

In applications where the viscoelastic model is used over a large range of characteristic times and as a consequence the choice of constitutive law goes to the Boltzmann convolution expression for the relaxation kernel. In these case most inverse problems discuss the recovering the memory kernels in the case of a *homogeneous* solids (see [17, 20, 28, 36]). However it is not simple for defects identification problems dealing with discontinuities in solids. For general papers on viscoelasticity theory, one can refer to [19, 21, 22]. For experimental determination of constants, we refer to [33].

In this paper we propose to discuss the crack identification problem in the particular case of the Zener model of

H. D. Bui · A. Constantinescu · E. Grasso
Laboratoire de Mécanique des Solides (CNRS UMR 7649),
Department of Mechanics, Ecole Polytechnique,
91128 Palaiseau cedex, France
e-mail: hdb@lms.polytechnique.fr

A. Constantinescu
e-mail: constant@lms.polytechnique.fr

E. Grasso
e-mail: grasso@lms.polytechnique.fr

H. D. Bui
LaMSID/CNRS (UMR 2932), EDF, Clamart 92141, France

S. Chaillat
College of Computing, Georgia Institute of Technology,
266 Ferst Drive, Atlanta, GA 30332-0765, USA
e-mail: stephanie.chaillat@cc.gatech.edu

linear viscoelasticity. This constitutive model has previously been considered for example in [27] in the case of rolling contact, in [10] for the cyclic modelling of polyamide fibre straps or in Sack et al. [32] and in Wuerfel et al. [35] for medical applications in soft tissues.

The problem of identifying a crack from overspecified data has received a lot of attention in the inverse problem community in the last two decades. Most of the results were obtain for the electric conductivity problem already discussed by Friedman and Vogelius in [25]. Later Bryan and Vogelius [11] and Alessandrini [2] discussed the uniqueness of the crack determination for single or multiple crack systems under a small number of measurements. Other aspects were also discussed by Alessandrini in different papers: the stabilty of the solution with respect to measurements was discussed in [1, 2]. However the techniques used in this paper is different from the preceeding citations and it is based on the reciprocity principle and more precisely on the symmetry lost (or loss of reciprocity) [12]. Different planar crack identification problems using this technique have already been discussed in [6, 7].

This paper starts with the presentation of the equivalence between elasticity and viscoelasticity under the condition of low frequency as exploited in [18] for a boundary integral equation approach. This framework will be applied for the identification of planar crack problem using boundary data. Different mathematical aspects of the inversion are addressed, particularly the identifiability of a planar crack in a 3D bounded solid, using exact boundary data, without considering numerical aspects. The main result for determining the crack plane in viscoelasticity is a direct method to compute the normal and location of the plane and also the complete crack extension in the crack plane. The zero crossing method introduced in our previous works appears to be a very simple proof of the identifiability of the normal and the crack plane.

2 A visco-elastic model

2.1 Stress–strain law

Various rheological models, generalization of the spring dashpot networks, are used for the representation of the viscoelastic behavior of a material [19, 26]. Within the most simple and popular ones, we count the Kelvin-Voigt model which is suited for solids and the Maxwell model used for fluids.

The rheological model used in this paper is a Zener one with a dashpot impedance η and elastic constants k_0 and k_1 as represented schematically in Fig. 1. One can characterize the behaviour of the model at very slow or vary large loading rates. If the strain rate goes to zero, i.e. in an infinitesimal slow loading when $\dot{\epsilon} = 0$, the dashpot has no effect and the model has a "delayed modulus" and is equivalent to two springs connected in series. For instantenous loading, conducting to large strain rates, i.e. if $\dot{\epsilon} = \infty$, then the dashpot is blocked and it the model exhibits an instantaneous modulus.

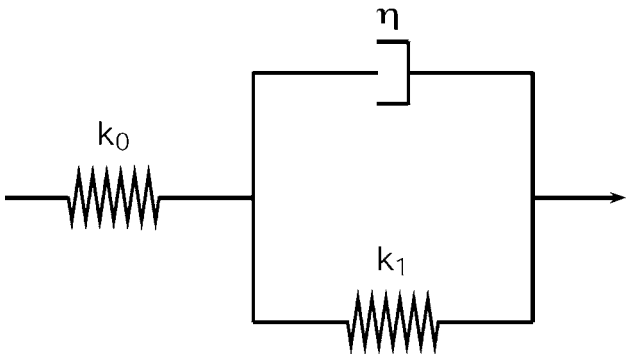

Fig. 1 Zener model of visco-elasticity

The usual formulation of isotropic visco-elastic law is given by the Boltzmann functional representation of the relaxation kernel:

$$\sigma_{ij}(t) = \int_0^t \lambda(t-\tau)\delta_{ij}\dot{\epsilon}_{kk}(\tau)d\tau + \int_0^t 2\mu(t-\tau)\dot{\epsilon}_{ij}(\tau)d\tau \quad (1)$$

with λ(t) and μ(t) being relaxation functions.

The Zener constitutive law is given by the differential equation:

$$\frac{1}{\eta}\boldsymbol{\sigma} + \dot{\boldsymbol{\sigma}} = \Lambda_\infty : \left(\frac{1}{\gamma}\epsilon + \dot{\epsilon}\right) \quad (2)$$

where $\Lambda_\infty = \lambda_\infty I_2 \otimes I_2 + 2\mu_\infty I_4$ is the instantaneous elastic moduli tensor, defined by instantaneous Lame's constants λ_∞, μ_∞ and γ, η are respectively creep time and relaxation times.

It is important to understand that it is always possible to express Eq. 2 in the form Eq. 1 with exponential relaxation functions (by integrating Eq. 2 in time). However the opposite is not true, if Boltzmann's relaxation functions $\lambda(t)$ and $\mu(t)$ are not of the exponential type, as is the case in general.

As a consequence, the Boltzman functional representation of the relaxation kernel, i.e. Eq. 1 is more general than Zener's model. Moreover it is equivalent to a differential form model using various orders of time derivatives.

We further remark that in Eq. 2 the delayed modulus is η/γ times the instantaneous modulus.

In the sequel, we rewrite Eq. 2 in the form proposed by Goriacheva [27] with the using delayed elastic tensor $\boldsymbol{\Lambda}$ defined with respect to the Lame's moduli λ, μ as:

$$\boldsymbol{\sigma} + \beta\dot{\boldsymbol{\sigma}} = \boldsymbol{\Lambda} : (\epsilon + \alpha\dot{\epsilon}) \quad (3)$$

The coefficients α, β defined as:

$$\alpha = \frac{\eta}{k_1}, \quad \beta = \frac{\eta}{k_0 + k_1} \tag{4}$$

can easily be determined from the scheme in Fig. 1 as explained next. The 1D rheological model satisfies the following relations $\sigma = k_0\varepsilon_1 = \eta\dot{\varepsilon}_2 + k_1\varepsilon_2$ and $\varepsilon = \varepsilon_1 + \varepsilon_2$ where ε_1 is the strain of the first spring with stiffness k_0, and ε_2 is the strain of the second spring with stiffness k_1. Eliminating ε_1 and ε_2 we obtain the stress strain law $\sigma + \frac{\eta}{k_0+k_1}\dot{\sigma} = \frac{k_0k_1}{k_0+k_1}(\varepsilon + \frac{\eta}{k_1}\dot{\varepsilon})$, in which $(k_0k_1)/(k_0 + k_1)$ is exactly the overall delayed stiffness E. Consequently $\sigma+\beta\dot{\sigma} = E(\varepsilon + \alpha\dot{\varepsilon})$. Equation 3 is nothing but the formal generalization of the 1D model, which has been introduced by Goriacheva [27].

We introduce the transformed stress, displacement and strain

$$\begin{cases} \sigma^* & = \sigma + \beta\frac{\partial\sigma}{\partial t} \\ u^* & = u + \alpha\frac{\partial u}{\partial t} \\ \epsilon^* & = \epsilon + \alpha\frac{\partial\epsilon}{\partial t} \end{cases} \tag{5}$$

The tensors σ* and ε* are linked by the constitutive equation of isotropic elasticity with the Lame coefficients λ and μ of the delayed moduli

$$\sigma^* = \Lambda : \epsilon^* \tag{6}$$

With $\boldsymbol{u}(\boldsymbol{x},t) = \boldsymbol{v}(\boldsymbol{x})\cos(\omega t)$ the displacement rate $\dot{\boldsymbol{u}}(\boldsymbol{x},t)$ is dephased of $\pi/2$. Using Eq. 5, we obtain $\boldsymbol{u}^*(\boldsymbol{x},t) = \boldsymbol{v}(\boldsymbol{x})(\cos(\omega t) - \alpha\omega\sin(\omega t))$. Defining the angle ψ such that $\tan\psi = \alpha\omega$ ($0 \le \psi < \pi/2$, i.e. $\cos\psi \neq 0$) it follows

$$\boldsymbol{u}^*(\boldsymbol{x},t) = \frac{\boldsymbol{v}(\boldsymbol{x})}{\cos(\psi)}\cos(\omega t + \psi) \tag{7}$$

It is now clear that variables $\boldsymbol{u}^*$ and $\boldsymbol{u}$ are out of phase of angle ψ but have the same circular frequency ω. Then, suppose that $\sigma(\boldsymbol{x},t) = w(\boldsymbol{x})\cos(\omega t + \theta)$, we obtain $\sigma^*(\boldsymbol{x},t) = w(\boldsymbol{x})[\cos(\omega t + \theta) - \beta\omega\sin(\omega t + \theta)]$. Defining in the same manner the angle ϕ such that $\tan\phi = \beta\omega (0 \le \phi < \pi/2)$ it follows:

$$\sigma^*(\boldsymbol{x},t) = \frac{w(\boldsymbol{x})}{\cos(\phi)}\cos(\omega t + \phi + \theta) \tag{8}$$

The variables σ* and $\boldsymbol{u}^*$ are known to satisfy the constitutive Eq. 6, so that they have to be in phase. It follows that $\psi = \phi + \theta$. Finally, σ and $\boldsymbol{u}$ have to be out of phase of $\theta = \psi - \phi$.

2.2 Remarks on the stress–strain law

Physically, most dissipative media, like soils and sand, can be considered as a mixture of fluid and solid particles so that their overall behaviors are also a combination of elastic law and viscous one. A good example is found in Wear Mechanics. The "third" body which represents the interface between two sliding solids, in the presence of wear and a fluid, behaves like an elastic solid in compression (normal to the interface) and as a viscous fluid in tangential shear, see [23, 24]. Both variables and their time derivatives are present in the physical law. Therefore a simple model for taking account of viscous dissipation consists in modifying a perfect law, for example $U = \lambda\text{grad}\ \varphi$ by adding terms involving derivatives with respect to time of various orders. The simplest one is suggested by Zener's model (Eq. 3), which includes time derivatives of order 1. When the rates are small, the relation between stress and strain $\sigma + \beta\dot{\sigma} = \Lambda : (\epsilon + \alpha\dot{\epsilon})$ is interpreted as a delayed response $\sigma = \Lambda : \epsilon$, while the relation between stress and strain rates, at high rates, corresponds to the rapid response $\beta\dot{\sigma} = \alpha\Lambda : \dot{\epsilon}$. Mixed relations existing between dominant terms, for example σ and $\alpha\dot{\epsilon}$, describe a viscous fluid behavior etc.

It is worth noting that the Zener model, like any other time dependent constitutive law, is especially valid for some time scale. Viscoelastic constitutive laws are obtained by a best fit with experiments or observations which can be made in some range of time at a fixed temperature. Therefore creep time α and relaxation time β can only be obtained by tests, although β is not often reported in the literature, perhaps because of difficulties to carry out relaxation tests. However there are some theoretical reasons for α and β to be of the same order, since according to Eq. 4, for one-dimensional model constants, k_0 and k_1 are comparable. Sometimes β is set to zero.

Consider the case of rocks. If the time of laboratory experiments is short, creep time is generally small, typically $\alpha \approx 0.001$–0.01 s, for rocks and also for metals at high temperature. Now consider a long term deformation of rocks of the continental crust which can undergo large deformation over millions of years (My). These rocks which are elastic in laboratory tests become viscoelastic in geological time, with more or less $\alpha \approx$, 1 My. Values for asphalt coating of roads are $\alpha \approx$ 0.1–10 s for the temperature in the range [0, 50°C]. Small values of creep time in laboratory tests $\alpha \approx$ 0.01–1 s are known for rubber like materials (rubber, plastics, etc) [34]. Smaller values of creep time $\alpha \approx 10^{-7}$–10^{-5} s are reported for $YBa_2Cu_3O_7$ oxide ceramic [31].

2.3 Equation of motion

The quantities σ* and $\boldsymbol{u}^*$ which are linked by the elastic law, are now shown to satisfy the equation of motion approximately. The assumed forms of fields σ and $\boldsymbol{u}$ are compatible with the equation of motion $\text{div}\sigma - \rho\ddot{\boldsymbol{u}} = 0$ if and only if the out of phase angle θ is very small. More precisely, the modification introduced in the dynamic equation by the phase difference between σ and $\boldsymbol{u}$ is

proportional to $\rho\omega^2\theta$. Since for small θ, we have $\theta \approx |\alpha - \beta|\omega$ and thus $\rho\omega^2\theta \approx \rho\omega^3|\alpha - \beta|$, where α and β are defined by Eq. 4 using $\boldsymbol{u}(\boldsymbol{x},t) = \boldsymbol{v}(\boldsymbol{x})\cos\omega t$. It follows that

$$\text{div } \sigma^* - \rho\ddot{\boldsymbol{u}}^* = \rho(\beta - \alpha)\partial_t\ddot{\boldsymbol{u}} \approx \rho\omega^3|\alpha - \beta|\|\boldsymbol{v}\|$$

The latter term can be neglected in comparison with $\rho\omega^2\|\boldsymbol{v}\|$ if and only if

$$\theta \approx |\alpha - \beta|\omega \ll 1 \tag{9}$$

Therefore, the frequency of the experiment must be much less than the limit frequency $\omega_1 = 1/|\alpha - \beta|$. The static case $\omega = 0$ obviously satisfies the latter condition. Since $|\alpha - \beta|$ is proportional to the viscosity coefficient η, the lower the coefficient η, the higher the limit frequency ω_1 (in solid mechanics η is indeed small, so that ω_1 is large). Also ω_1 is large when $|\alpha - \beta|$ is small for some rheological models. For example, rubber like materials have $\alpha \approx 0.01$–1 s. Assuming that $\beta = 0$, we can take $\omega_1 = 1$–100 hz. The limit frequency depends on the nature of materials. For values of $\omega_1 < 1$ hz, the quasi-static assumption may be used in practice.

Finally, provided that $\omega \ll \omega_1$, the change of functions using $\boldsymbol{u}^*$ and σ^* leads to the same elastodynamic equation $\text{div } \sigma^* + \rho\omega^2\boldsymbol{u}^* = 0, \sigma^* = \Lambda : \epsilon^*$. This correspondence between viscoelasticity and elasticity making use of a real Helmholtz equation has been exploited in [18] for a new approach of real boundary integral equation. In what follows, we address the identifiability of a planar crack in viscoelasticity. We show that the solution of crack inverse problems in viscoelasticity reduces to the solution of an inverse problem for the vectorial Helmholtz equation. Let us remark that the antiplane loading is a particular case of the general model considered in this paper. In the dynamic antiplane case, we shall deal with a crack inverse problem for the scalar acoustic Helmholtz equation, for which we can use the solutions provided by Alves and Ha Duong [4, 5] and Ben Abda et al. [9].

Let us also remark that crack inverse problems in the quasistatic case $k = 0$ have been widely considered in the literature, see [2, 3, 6, 8, 13, 15]. These solutions can be used for crack inverse problems in 2D, 3D viscoelasticity, via the transformed displacements and transformed stress.

3 Identification of a planar crack for the vectorial Helmholtz equation

We consider a time harmonic loading on a 3D viscoelastic solid Ω weaken by a planar crack F, with frequency ω. The elastodynamic equation for the transformed displacement $\boldsymbol{u}^*$ becomes, with $k^2 = \rho\omega^2$

$$\mu\text{div}(\text{grad } \boldsymbol{u}^*) + (\lambda + \mu)\text{grad}(\text{div } \boldsymbol{u}^*) + k^2\boldsymbol{u}^* = 0, \text{ in } \Omega \setminus F \tag{10}$$

Let us denote the boundary transformed displacement and transformed stress vector by $\boldsymbol{u}^* = \boldsymbol{u}^d$ and $\sigma^* \cdot \boldsymbol{n} = \boldsymbol{T}^d$ respectively. These boundary vectors are used as data for the inverse problem. The planar crack is stress free, $\sigma^* \cdot \boldsymbol{n} = 0$ on $F^{\pm}$. The boundary of the cracked solid consists of the external boundary $\partial\Omega_{\text{ext}}$ and internal boundaries $F^{\pm}$. The crack geometry is denoted by F, with the normal $\boldsymbol{n}$ chosen as $\boldsymbol{n} = \boldsymbol{n}^- = -\boldsymbol{n}^+$.

The method of solution is based on the use of various adjoint fields $\boldsymbol{w}$ satisfying the same Helmholtz equation over the uncracked domain Ω

$$\mu\text{div}(\text{grad } \boldsymbol{w}) + (\lambda + \mu)\text{grad}(\text{div } \boldsymbol{w}) + k^2\boldsymbol{w} = 0, \text{ in } \Omega \tag{11}$$

Multiply Eq. 10 by $\boldsymbol{w}$ and Eq. 11 by $\boldsymbol{u}^*$, then substract the results, integrate over the cracked domain and finally transform the volume integral into boundary integrals. Using the continuity of $\boldsymbol{w}$ across F, the stress free condition on $\sigma^*.\boldsymbol{n} = 0$ on $F^{\pm}$, and denoting by $[\![\boldsymbol{u}^*]\!] = \boldsymbol{u}^{*+} - \boldsymbol{u}^{*-}$ the crack displacement jump, we can derive the following variational equation

$$\int_F [\![\boldsymbol{u}^*]\!] \cdot \sigma[\boldsymbol{w}] \cdot \boldsymbol{n} = \int_{\partial\Omega_{\text{ext}}} (\boldsymbol{w} \cdot \sigma[\boldsymbol{u}^*] \cdot \boldsymbol{n} - \boldsymbol{u}^* \cdot \sigma[\boldsymbol{w}] \cdot \boldsymbol{n})dS = R(\boldsymbol{w}; \boldsymbol{T}^d, \boldsymbol{u}^d) \tag{12}$$

for *any* adjoint field $\boldsymbol{w}$. In Eq. 12 $R(\boldsymbol{w}; \boldsymbol{T}^d, \boldsymbol{u}^d)$ denotes the second integral in which boundary data have been inserted. R is called the reciprocity gap functional introduced in our previous works on the identifiabilty of a planar crack in 3D [6, 12, 14, 16].

We now choose particular adjoint fields in order to determine first the normal to the crack plane, then the location of the crack plane and finally the crack geometry.

3.1 The normal to the crack plane

We consider an adjoint *S*-wave field $\boldsymbol{w}$ depending on two orthogonal vectors of the same norm, $\boldsymbol{p} \cdot \boldsymbol{p}^{\perp} = 0, \quad \|\boldsymbol{p}^{\perp}\| = \|\boldsymbol{p}\|$

$$\boldsymbol{w} = \sin(\boldsymbol{x} \cdot \boldsymbol{p}^{\perp})\boldsymbol{p} \tag{13}$$

The adjoint field $\boldsymbol{w}$ satisfies the wave equation if these orthogonal vectors are on the sphere S of radius $k/\sqrt{\mu}$ or

$$\|\boldsymbol{p}\|^2 = \frac{k^2}{\mu} \tag{14}$$

Inserting Eq. 13 in Eq. 12 we get

$$\mu\Big[(p_j^{\perp}n_j)p_i + (p_jn_j)p_i^{\perp}\Big]\int_F [\![u_i^*]\!]cos(\boldsymbol{x}\cdot\boldsymbol{p})dS = R(\boldsymbol{p},\boldsymbol{p}^{\perp}) \tag{15}$$

where for brevity we set $R(\boldsymbol{p},\boldsymbol{p}^{\perp}) := R(\boldsymbol{p},\boldsymbol{p}^{\perp};\boldsymbol{T}^d,\boldsymbol{u}^d)$.

Function $R(\boldsymbol{p},\boldsymbol{p}^{\perp})$ vanishes when vectors $\boldsymbol{p},\boldsymbol{p}^{\perp}$ are orthogonal to $\boldsymbol{n}$, i.e when they are parallel to the crack plane. Thus vector $\boldsymbol{q} = \boldsymbol{p}\times\boldsymbol{p}^{\perp}/\|\boldsymbol{p}\|$ on the same sphere S is along $\boldsymbol{n}$. Therefore, because of a priori assumption on a single planar crack, the normal direction is uniquely determined by a zero crossing method. The solutions $\pm\boldsymbol{n}$ correspond to the poles or the zeros of function $R(\boldsymbol{q})(= R(\boldsymbol{p},\boldsymbol{p}^{\perp}))$ of $\boldsymbol{q}$ on the sphere S, for any $\boldsymbol{p},\boldsymbol{p}^{\perp}$ in the equatorial plane, Fig. 2.

3.2 The location of the crack plane

Once the normal has been obtained, we consider Ox_3 along the normal. The crack plane is defined by $x_3 - D = 0$ with D to be determined by a zero crossing method, using a P-wave adjoint field depending on a scalar parameter η

$$\boldsymbol{w}(\boldsymbol{x};\eta) = \cos(q(x_3-\eta))\boldsymbol{e}^3 \tag{16}$$

Field $w(\boldsymbol{x};\eta)$ satisfies the wave equation if we take

$$q = \frac{k}{\sqrt{\lambda+2\mu}} \tag{17}$$

Inserting Eq. 17 into Eq. 12 with $x_3 - D = 0$ on the crack F, we obtain

$$-q(\lambda+2\mu)\sin(q(D-\eta))\int_F [\![u_3^*]\!]dS_x = R(\eta) \tag{18}$$

If we choose k such that the wave length $2\pi/q > L$ is larger than the size L of Ω, then according to Eq. 18 the reciprocity gap $R(\eta) := R(\boldsymbol{w}(\eta);\boldsymbol{T}^d,\boldsymbol{u}^d)$ which is function of parameter η has a unique zero $\eta = D$ corresponding to the crack plane location. The other zeros of $\sin(q(D-\eta)) = 0$ correspond to non physical planes outside the solid.

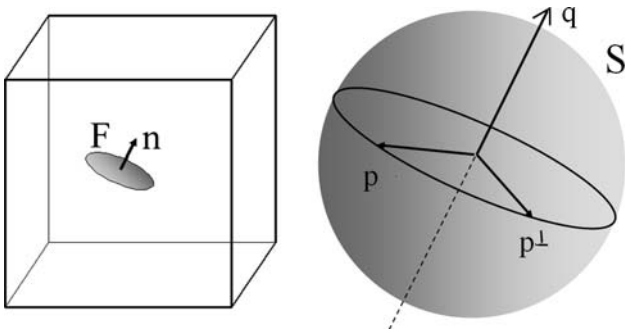

Fig. 2 Vectors $\boldsymbol{q} = \boldsymbol{p}\times\boldsymbol{p}^{\perp}/\|\boldsymbol{p}\|$ such that $R(\boldsymbol{q}) = 0$ are along the pole axis which is parallel to the normal to the crack plane

3.3 Identification of the crack geometry

Since the crack plane is determined, it is convenient to take the origin on the crack plane $\Pi = Ox_1x_2$. We need to introduce adjoint fields which depend on 2D real vectors $\boldsymbol{p} = (p_1,p_2,0)$ of arbitrary norm. We introduce two complex vectors

$$Z(\boldsymbol{p})^{\pm} = \boldsymbol{p} \pm i\gamma\|\boldsymbol{p}\|\boldsymbol{e}^3 \tag{19}$$

and two vector fields

$$w^{\pm}(\boldsymbol{x},\boldsymbol{p}) = \nabla_x\exp(-iZ(\boldsymbol{p})^{\pm}.\boldsymbol{x}) \tag{20}$$

Fields $w^{\pm}$ satisfy the vectorial Helmholtz equation if

$$\gamma^2 = 1 - \frac{k^2}{(\lambda+2\mu)\|\boldsymbol{p}\|^2} \tag{21}$$

The adjoint displacement and adjoint normal stress are then given respectively by

$$\boldsymbol{v}(\boldsymbol{x},\boldsymbol{p}) = \boldsymbol{w}^+(\boldsymbol{x},\boldsymbol{p}) + \boldsymbol{w}^-(\boldsymbol{x},\boldsymbol{p}) \tag{22}$$

$$\sigma_{33}[\boldsymbol{v}] = 2(\lambda(\gamma^2-1)+2\mu\gamma^2)\|\boldsymbol{p}\|^2\exp(-i\boldsymbol{p}\cdot\boldsymbol{x}) \tag{23}$$

The reciprocity gap functional becomes

$$2(\lambda(\gamma^2-1)+2\mu\gamma^2)\|\boldsymbol{p}\|^2\int_F [\![u_3(\boldsymbol{x})]\!]\exp(-i\boldsymbol{p}\cdot\boldsymbol{x})dS_x = R(\boldsymbol{u}^d,\boldsymbol{T}^d;\boldsymbol{v}(\boldsymbol{p})) \tag{24}$$

The Fourier transform of the jump $[\![u_3]\!]$ is completely determined and thus the jump is given by

$$[\![u_3(\boldsymbol{x})]\!] = \frac{1}{(2\pi)^2}\int_{\Pi(p_3=0)} \frac{\exp(+i\boldsymbol{p}\cdot\boldsymbol{x})}{2(\lambda(\gamma^2-1)+2\mu\gamma^2)\|\boldsymbol{p}\|^2} \times R(\boldsymbol{u}^d,\boldsymbol{T}^d;\boldsymbol{v}(\boldsymbol{p}))dp_1dp_2 \tag{25}$$

Therefore the crack geometry is explicitly identified by the support of the jump function $u_3(x_1, x_2)$ in the whole plane Π.

4 Conclusions

In this paper we have considered a particular form of viscoelastic constitutive equations described by a first order differential equation of the Zener type.

For low frequencies of the load, the constitutive equation of the transformed stress and strain for viscoelasticity, is approximately the same as in elasticity while it is strictly equivalent to elasticity in quasistatic loadings. These transformed functions are simpler than functions obtained by Fourier transforms of fields.

The main advantage of the method is to allow inverse problems for crack identification to be solved in a straightforward manner by considering existing solutions to

the same inverse problem for the Helmholtz equation (in dynamics) or the elastic equation (in quasistatics). For the planar crack detection, a new result for identifying the crack normal, the crack plane and geometry has been presented for the elastic Helmholtz equation.

Methods of solution to inverse problems considered in this paper are based on the study of the zeros of the functional R. By choosing adjoint fields depending on adequate parameters explicitly, we are dealing with *function* R of these parameters. The detection of crack is obtained by studying the transition between zero and non zero values of function R while varying the parameters of the adjoint field. The reciprocity gap R is indeed a defect indicator.

References

1. Alessandrini G (1993) Stable determination of a crack from boundary measurements Auteur(s)/Author(s). Proc R Soc Edinb Sect A Math 123(3):497–516
2. Alessandrini G, Diaz Valenzuela A (1996) Unique determination of multiple cracks by two measurements. SIAM J Control Optim 34:913–921
3. Alessandrini G, Di Benedetto E (1997) Determining 2-dimensional cracks in 3-dimensional bodies: uniqueness and stability. Indiana Univ Math J 46:1–82
4. Alves CJS, Ha-Duong T (1999) Inverse scattering for elastic plane waves. Inverse Probl 15:91–97
5. Alves CJS, Ha-Duong T (1997) On inverse scattering by screen. Inverse Probl 13:1161–1176
6. Andrieux S, Ben Abda A, Bui HD (1999) Reciprocity principle and crack identification. Inverse Probl 15:59–65
7. Andrieux S, Ben Abda A (1996) Identification of planar cracks by complete overdetermined data: inversion formulae. Inverse Probl 12:553–563
8. Andrieux S, Ben Abda A (1992) Identification de fissures planes par une donnee de bord unique: un procede direct de location et d'identification. C R Acad Sci Paris 315(I):1323–1328
9. Ben Abda A, Delbary F, Haddar H (2005) On the use of the reciprocity-gap functional in inverse scattering from planar cracks. Math Models Methods Appl Sci 115:1553–1574
10. Bles G, Nowacki WK, Tourabi A (2009) Experimental study of the cyclic visco-elasto-plastic behaviour of a polyamide fibre strap. Int J Solids Struct 46:2693–2705
11. Bryan K, Vogelius M (1992) A uniqueness result concerning the identification of a collection of cracks from finitely many electrostatic boundary measurements. SIAM J Math Anal 23:950–958
12. Bui HD (1994) Inverse problems in the mechanics of materials: an introduction. CRC Press, Boca Raton
13. Bui HD, Constaninescu A, Maigre H (2005) The reciprocity gap functional for identifing defects and cracks. In: Mroz Z, Stavroulakis GE (eds) Parameter identification of materials and structures. CISM course and lecture, vol 469. Springer, New York
14. Bui HD, Constaninescu A, Maigre H (2005) An exact inversion formula for determining a planar fault from boundary measurement. J Inv Ill-Posed Probl 13:553–565
15. Bui HD (2006) Fracture Mechanics. Inverse problems and solution. Springer, New York
16. Bui HD, Constaninescu A, Maigre H (2005) Inverse acoustic scattering of a planar crack: closed form solution for a bounded solid. C R Acad Sci Paris 327:971–976
17. Catheline S, Gennisson JL, Delon G, Fink M, Sinkus R, Abouelkaram S, Culioli J (2004) Measuring of viscoelastic properties of homogeneous soft solid using transient elastography: an inverse problem approach. J Acoust Soc Am 116(6):3734–3741
18. Chaillat S, Bui HD (2007) Resolution of linear viscoelastic equations in the frequency domain using real Helmholtz boundary integral equations. Comptes Rendus de Mecanique 335:746–750
19. Christensen RP (1971) Theory of viscoelasticity—an introduction. Academic Press, London
20. Corones J, Karlsson A (1988) Transient direct and inverse scattering for inhomogeneous viscoelastic media obliqued incident SH mode. Inverse Probl 4(3):643–660
21. Del Piero G, Deseri L (1997) On the concepts of state and free energy in linear viscoelasticity. Arch Ration Mech Anal 1(38):138
22. Deseri L, Mares R (2000) A class of viscoelastoplastic constitutive models based on the maximum dissipation principle. Mech Mater 138(38):1–35
23. Dragon-Louiset M (2001) On a predictive macroscopic contact-sliding wear model based on micromechanical considerations. Int J Solids Struct 38:1625–1639
24. Dragon-Louiset M, Stolz C (1999) Approche thermodynamique des phenomenes d'usure de contact. C R Acad Sci Paris 327(IIb):1275–1280
25. Friedman A, Vogelius M (1989) Determining cracks by boundary measurements. Indiana Univ Math J 38:527–556
26. Flügge W (1975) Viscoelasticity. Springer, New York
27. Goriacheva IG (1973) Contact problem of rolling of a viscoelastic cylinder on a base of the same material. PMM 37:925–933
28. Janno J, Von Wolfersdorf L (1999) Inverse problems for identification of memory kernels in thermo- and poro-viscoelasticity. Math Methods Appl Sci 21(16):1495–1517
29. Muller M, Genisson JL, Deffieux T, Sinkus R, Philippe A, Montaldo G, Tanter M, Fink M (2007) Full 3D inversion of the viscoelasticity wave propagation problem for 3D Ultrasound elastography in breast cancer diagnosis. In: Ultrasonics symposium IEEE, pp 672–675
30. Phan-Thien N (2002) Understanding viscoelasticty. Springer, New York
31. Ren C, Ding SY, Zheng ZY, Qin MJ, Yao XX, Fu XY, Cai CB (1996) Dependence of the flux-creep time scale on sample size for melt-textured YbaCuO by ac-susceptibilty measurements. Phys Rev B 53(17):11348–11351
32. Sack I, Beierbach B, Wuerfel J, Klatt D, Hamhaber U, Papazoglou S, Martus P, Braun J (2009) The impact of aging and gender on brain viscoelasticity. Neuroimage 46:652–657
33. Soula M, Vinh T, Chevalier Y (1997) Transient responses of polymers and elastomers deduced from harmonic responses. J Sound Vib 205:185–203
34. van Vliet T (1999) Factors determining small deformation behavior of gel. In: Dickinson E, Rodriguez Patino JW (eds) Food emulsions and foam interfaces, interactions and stability, pp 307–317
35. Wuerfel J, Friedemann P, Beierbach B, Hamhaber U, Klatt, Papazoglou S, Zipp F, Martus P, Braun P (2009) MR-elastography reveals degradation of tissue integrity in multiple sclerosis. Neuroimage. doi:10.1016/j.neuroimage.2009.06.018
36. Xianyao C, Changjun C (1999) Inverse problem for the viscoelastic medium with discontinuous wave impedance. Appl Math Mech 20(11):1222–1229